Opto-chemical pH detection of Myocardial Ischaemia using Fluorescent Hydrogels

De Graaf, Ger; Vriesendorp, Maurits Frans; Hassan, Amin; French, Patrick James

DOI
10.1109/JSEN.2022.3166709

Publication date
2022

Document Version
Accepted author manuscript

Published in
IEEE Sensors Journal

123 4

Opto-chemical pH detection of Myocardial Ischaemia using Fluorescent Hydrogels

Ger de Graaf, *Member, IEEE,*, Maurits Frans Vriesendorp, Amin Hassan and Patrick James French, *Fellow, IEEE*

***Abstract*— In this research fluorescent optochemical pH probes for the detection of ischaemia have been investigated. Myocardial ischaemia is the most prominent risk during heart surgery. During open heart surgery the heart is temporarily arrested and, since there no blood flowing, oxygen supply and removal of waste products is stopped and heart cells can be damaged. In this paper we propose a novel method to monitor the condition of the heart by placing optochemical pH sensors on several strategic places around the heart during surgery. Low cost opto-chemical pH sensors, using a HPTS (8-hydroxy-1,3,6-pyrene trisulfonic acid trisodium salt) fluorescent dye encapsulated in a thin bio-compatible hydrogel layer, were investigated for this application. Our research started with an extensive optical characterization of several types of hydrogel layers at different pH levels. Secondly a reflection probe prototype using several of these layers was designed, built and tested. Dual wavelength excitation and ratiometric detection of the fluorescent signals was used to detect the pH level. Typical output signals of 35% to 53% per pH in the range from 6.5-8.0 pH have been measured and a response time of typically 400 seconds was obtained for the prototypes. Finally based on our measurements on the HPTS layers and the reflection probe we propose an improved type of pH probe for the detection of ischaemia during open heart surgery.**

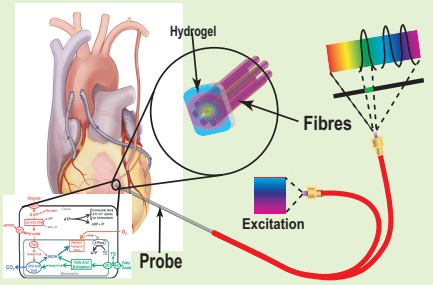

***Index Terms*— Fluorescence, ischaemia, hydrogel, optical pH probe, HPTS, pyranine, fluorescent dye, dual wavelength excitation, ratiometric detection.**

I. Introduction

DURING open heart surgery the heart is temporarily arrested by administering cardioplegia. Cardioplegia is a pharmacological solution that ”pauses” the heart muscle cells, resulting in a Cardioplegia Induced Cardiac Arrest and the function of the heart and lungs is taken over by a heart-lung machine. During the cardiopulmonary bypass no oxygenated blood is going to the heart and a change in the metabolism of the heart muscle cells occurs. The middle layer of the heart wall (myocardium) is composed of cardiomyocytes, heart muscle cells [1]. For a given condition of the heart an initial amount of cardioplegia is administered [2], but heart muscle cells may become permanently damaged if the cardioplegia does not reach all cells [3]. Myocardial damage (ischaemia) is one of the most common causes of morbidity and mortality after heart surgery [4]. The number of patients with myocardial damage can vary between 2-10% after coronary artery bypass surgery [5] and 29% of aortic valve replacement [6]. When the condition of the heart is better monitored on ischaemia symptoms, the degree of the injury and mortality can be decreased. The next section briefly discusses myocardial ischaemia followed by short overview of the methods for measuring the heart condition during a Cardioplegia Induced Cardiac Arrest.

Ger de Graaf and Paddy French are with the Department of Electrical, Mathematics and Computer Engineering, Delft University of Technology, 2622 CD Delft, The Netherlands e-mail: Ger.deGraaf@tudelft.nl .

Amin Hassan is with the Else Kooi Lab., Faculty of Electrical Engineering, Mathematics and Computer Science, Delft University of Technology, 2628 CT Delft, The Netherlands e-mail: H.M.AminHassan@tudelft.nl .

Maurits Vriesendorp is with the Department of Biomedical Engineering, Delft University of Technology, 2622 CD Delft,

Manuscript received November 30, 2021; revised December 30, 2021.

II. Myocardial ischaemia

Oxygen is needed for the metabolism of the cardiomyocytes and ischaemia occurs as a consequence of an imbalance between oxygen supply and oxygen demand. The mitochondria of the cardiomyocyte cannot produce enough energy (Adenosine triphosphate, ATP) because of a lack of oxygen and they switch to anaerobic glycolysis to produce energy. This change of metabolism causes a negative energy balance in the cardiomyocyte and uses high energy reserves. Cardioplegia plays an essential role in reducing the energy demand of the cardiomyocytes thereby reducing damage [3] [7]. The anaerobic glycolysis causes an increase in lactic acid, which will immediately break down into lactate and hydrogen atoms. The increase of the acidity in the cardiomyocytes causes the intracellular pH (pHi) to drop. Besides an insufficient oxygen supply, ischaemia is also associated with reduced availability of nutrients and the inadequate removal of metabolic waste products. Since there is no blood flow, CO_2 can not be transported away and will accumulate in the cell. Pischke et

al. [8] showed that there is a correlation between the tissue CO_2 (P_tCO_2), the tissue lactate and tissue pH. As described by [9] the physical quantities directly related to the ischaemia of the heart cells are PCO_2, StO_2, Lactate, and pH. Based on our literature study [10] we have selected pH measurement as the most promising technique for detecting ischaemia.

III. Detection of ischaemia by pH measurement

A drop of intracellular pHi immediately starts after ischaemia occurs [11]. During ischaemia the red blood cells in the intravascular space are used to accept protons. This can partially delay the decrease of the pHi and results in a less intracellular acidification as compared with the extracellular pH (pHe) [12] protecting the cells against hypoxic, ischaemic and toxic injuries [13]. Both the drop of extracellular pH and intracellular pH are parameters that can be measured. The potential of measuring pH during cardiac surgery was shown in 1985 by [14]. In a study of [15] three glass pH-sensors were placed on the heart to monitor the pH level during cardioplegia. A clear drop of pH of the posterior tissue in comparison with the anterior tissue was observed, indicating that there was a problem with the cardioplegia. Khuri and Marston [14] and Khabbaz et al. [15] showed the capability to monitor ischaemia in the heart with pH measurements. Pischke et al. [16] measured the pH and the accumulation of CO_2. Multiple studies have shown the direct correlation between pH and lactate, e.g. Atkins et al. [17] and Nichols et al. [18]. Most research on pH sensing in the body is in the field of blood measurements, since this would make the blood gas analysers and blood tests redundant. Good results have been achieved in vitro, but in vivo testing is still a challenge [9].

IV. Requirements during open heart surgery

In the operating theatre it is important for the surgeon to monitor the ischaemia real-time, in vivo, reliable and safe. The system should be robust, easy to handle and should not be in the way during the operation. Several sensors are needed to measure ischaemia locally. Khabbaz et al. [15] showed that at least three sensors in the flow areas of all coronary arteries are needed for reliable measurements, however surgeons prefer to have data from more locations around the heart. There are several methods to measure pH and there are three main challenges when measuring in vivo during a Cardioplegia Induced Cardiac Arrest. First of all the environment should be aqueous enough to enable the transfer of hydrogen ions from the myocard, the main muscle tissue of the heart, to the outer epicardium/pericardium layer. Secondly, instead of blood the coronary arteries are filled with cardioplegia, consisting of many ions, to depolarise the cells. These ions change the ionic strength inside the heart. The concentration of these ions depends on the technique and the type of cardioplegia used. In vivo tests are needed to demonstrate the effect of cardioplegia on the proposed sensor system. Finally, temperature is known to vary during operations, and since pH values are temperature dependent, temperature sensing and compensation needs to be implemented. Taking into account the considerations above, we have selected optochemical detection of real time changes in pH in the range between 6.5 and 8 on several locations around the heart. These measurements need to be combined with temperature measurements.

V. Optochemical pH sensing

Optochemical sensing of tissue and blood pH is discussed extensively in a review article by [9]. The most promising approaches are a device using a 400µm multimode fibre with 37 cores coated with a sol-gel with encapsulated HPTS (8-hydroxy-1,3,6-pyrene trisulfonic acid trisodium salt) described by [19] and a hydrogel-based device using two fluorophores (5(6)-FAM and Porphyrin) by [20]. For in-line blood pH measurements a sensor using HPTS encapsulated in microbeads has been presented by Cattini et al. [21]. Although sol-gels are chemically, photochemically and mechanically more stable [22] they are much more complex to fabricate than hydrogels. In this work a hydrogel was selected as the base material for extracellular opto-chemical detection of pH since hydrogels allow a simpler chemical and more iterative design process.

VI. pH Sensitive Hydrogels

HydroMed D4 does not need activation and is one of the most used and proven bio-compatible hydrogels. HydroMed can be developed by dissolving in ethanol and mixed with an indicator. Phenolic luminophores like HPTS have a phenol group which is part of the chromophoric system. This group can be phenol and phenolates. If the phenolate is photo excited it causes fluorescence. Fluorescence decreases if the pH drops because there is less absorption of the phenolate form. HPTS (Pyranine) is a commonly used indicator and was selected since it has a very high sensitivity to pH, a large Stokes shift and does not need advanced chemical processing. A disadvantage of HPTS is that it is prone to bleach and affects the solutions ionic strength, which influences pH sensitivity. Photobleaching is the irreversible destruction of the fluorophore and is best prevented by optimizing the optical path to maximize signal so the lowest possible level of illumination can be used. The influence of the pKa of the HPTS layer on the ionic strength of the test solution should be kept in mind when measuring pH sensitivity. Stored under proper conditions, typical lifetimes of hydrogel layers with HPTS of more than 120 days have been reported [23].

A. Fabrication of the sensing layers

The processing steps for the fabrication of the samples are illustrated in Fig. 1. The left-hand side shows the process of filling the microbeads with HPTS. A dye immobiliser has to be used since the HPTS can not be mixed directly with the hydrogel. For this AmberChrom 1x8 is used as an anion exchange resin [24] and [21]. This is a relatively simple method to immobilise the HPTS in the hydrogel although it affects the ionic strength of the material. After this 1 gram of crushed Hydromed D4, 1 ml of demineralised water, and 9 ml of ethanol (96%) were poured together and mixed for 6 hours until the Hydromed D4 fully dissolved into the ethanol. Meanwhile, water was extracted from the HPTS microbeads

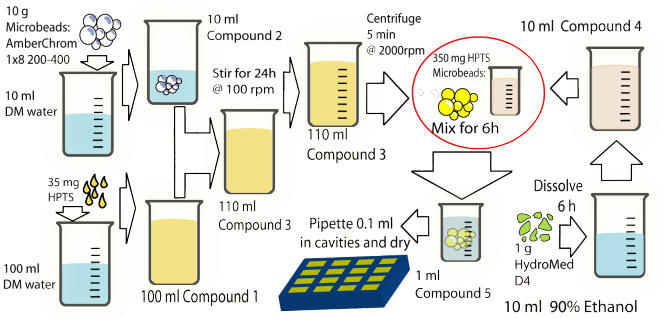

Fig. 1. Hydrogel samples fabrication process.

Sample	A	B	C	D	units
Thickness	1	1	0.5	0.5	[mm]
HydroMed D4	0.1	0.1	0.1	0.1	[g/ml]
Microbeads	1	1	1	1	[g/ml]
HPTS	0	3.5	17.5	35	[mg/ml]
$d_p(\lambda = 405nm)$	5.00	0.77	0.87	1.32	[mm]
$d_p(\lambda = 475nm)$	5.02	2.91	1.781	1.46	[mm]
$d_p(\lambda = 525nm)$	7.06	10.2	5.23	6.25	[mm]
pKa	6.99	7.73	7.23	6.20	

d_p is the light penetration depth in the hydrogel, pKa is the negative log of the acid dissociation constant.

TABLE I
OVERVIEW OF THE MAIN SAMPLES USED.

and the HPTS microbeads were mixed with the hydrogel solution at a ratio of 1 ml of hydrogel to 350 mg of microbeads and stirred for one hour. The final steps in fabrication of the hydrogel are joining the HPTS microbeads with the Hydromed D4 hydrogel at ambient temperature. A batch of several hydrogel layers consisting of 1 g/ml Hydromed D4, 1 g/ml microbeads were fabricated from the hydrogel solutions. Table I shows the main data of the four main types of samples. Three different HPTS concentrations were used: Sample B = 3.5 mg/ml, C = 17.5 mg/ml, D = 35 mg/ml. Sample A was intended without any HPTS in the microbeads. However, due to contamination in the processing a few microbeads contained HPTS. The hydrogel solutions were diluted with 1 ml of ethanol before pouring them in containers of 0.5 and 1 mm height. A surgical knife was used to scrape off the excessive solution. Per solution 6 different samples were made for pH determinations. The fabricated hydrogel layers are relatively strong, flexible and can be handled easily during prototype development.

B. Hydrogel initial tests

For initial tests the samples were investigated using a Zeiss Axiomat microscope with a camera using the standard coaxial light source. In the photo of Fig. 2 the size differences of 37 to 75 microns, as given by the manufacturer, of the microbeads can be seen. An increasing yellow color, i.e. increasing absorption of blue light with increasing HPTS concentration has been observed also.

The hydrogels were tested by immersion into calibrated pH buffer solutions. A Schott Instruments Analytics LAB850 with an N64 probe was used to fabricate 40 different buffer solutions stepping up from pH = 6.2 until pH = 8.2. The pH

(a) Sample A (b) Sample D

Fig. 2. Camera photos showing microbeads.

sensitive fluorescence response was verified by illumination of the samples at wavelengths of $\lambda_l = 405$ nm and $\lambda_h = 475$nm using a Triax-180 monochromator and a CMOS camera. The images on the CMOS camera showed an increasing absorption of blue light with increasing HPTS concentration and green fluorescent light from the microbeads. During these initial experiments we have tried several concentrations of HPTS and selected the concentration of sample C because of the expected optimal response around pH=7. Sample B has a the highest response at a lower pH and sample D at a higher pH. Sample A was intended without any HPTS however some microbeads contained HPTS due to contamination. We have selected only two thicknesses (0.5 and 1.0 mm) to limit the amount of samples and scans at each pH level in the spectrometers. The effect of the layer thickness on the response time (diffusion constant) can be also estimated from the two layer thicknesses. The samples were stored in light-tight bottles in water.

VII. SENSING LAYER CHARACTERISATION

This section discusses the optical characteristics of the different hydrogel layers, followed by an investigation of the fluorescence of the samples. We examined two layer thicknesses, i.e. 1 mm for sample A and B and 0.5 mm for sample C and D. The spectrophotometer graphs shows the effect of the increasing concentration of HPTS in samples A, B, C and D on the absorption, fluorescence and the pKa of the samples.

A. Transmission and reflection of the hydrogels

The samples were fixed by taping them to microscopic glasses since, due to their hydrophilic nature when wet, they do not adhere to glass. They were submerged for 5 minutes in the prepared pH buffers. The layers ionic strength solutions of 150 mM were selected, since this matches the typical ionic strength of the human body. After 5 minutes, the samples were taken out of the buffer solution and excessive solution was removed with clean-room wipes. For each sample described in section VI-A these steps were repeated for six different pH buffers with an ionic strength of 150 mM. F or the 4 types of samples the optical properties of the layers were investigated using a Perkin Elmer Lambda-1050 spectrophotometer. The range was set from λ= 350 nm to 700 nm in steps of 5 nm. For transmission measurements a converging lens was put in front of the sample holder to collimate the light onto the sample. This lens created a focal area of of 25 mm^2 and using the align function, a white light beam was projected on the focal

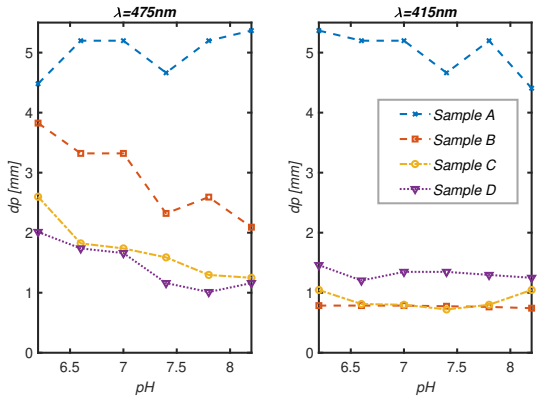

Fig. 3. Absorption depth for **λ**= 475 and 415 nm at different pH levels.

area. The total transmittance of the samples was measured by placing them in front of the entrance of the integrating sphere. A tungsten halogen light source and a double monochromator set-up with a common beam depolarizer, to correct for inherent instrument polarization, were used. Before measuring the samples, 0% and 100% transmission calibration steps were done. Fig. 4 shows the results of the selected samples. From the measured transmittance $T(\lambda)[\%]$ the absorbance $\alpha(\lambda)$ was calculated using Beer's law [25] as

$$\alpha(\lambda) = -log(T(\lambda)) = -log(\frac{T(\lambda)[\%]}{100}). \quad (1)$$

The absorption or penetration depth, i.e. the optical path length where the transmitted power decreases to $1/e$ or 36.8%, for different wavelengths can be written as

$$d_p(pH, \lambda) = \frac{-L}{log(T(pH, \lambda))} \quad (2)$$

where L is the sample thickness. The penetration depth of photons at different pH values can be derived from the measured transmittance of the samples. As shown in Fig. 4 sample A (low HPTS) shows a high transmission, i.e. low absorption, above 510 nm and only 2.5% decrease over the whole pH range. The transmission typically starts to decrease below λ= 440 nm. Some small artifacts can be seen at λ_h= 475 and λ_l= 405 nm in sample A due to the contamination with HPTS. Samples C and D have a higher transmittance due to a lower thickness. Fig. 3 shows the extracted data from Fig. 4 at the two optical resonant modes (λ = 475 and 415 nm) of the HPTS dye. At λ_l= 405 nm the measured absorption depth d_p does not significantly change with the pH, while at λ_h= 475 nm all samples with HPTS show a decreasing absorption depth with increasing pH. The increasing absorption at this wavelength indicates that the transmittance of the HPTS dye at λ_h can be used for pH detection. A better quality signal may be expected from detection the amount of fluorescence resulting from the resonant excitation of the dye material, as will be shown in the next section.

B. Fluorescence microscopy

In the next section the fluorescence of the sample layers at different wavelengths and at several pH levels will be investigated. Fig. 5 shows some sample images from a Zeiss Axiovert 200-M fluorescence microscope using an excitation filter of 472/30 and an emission filter of 520/35 (GFP-3035B filter) at different pH values.

Sample A was intended without any HPTS in the microbeads. However, due to contamination in the processing some microbeads contained HPTS as can be seen in Fig. 5 where some fluorescence can be observed. Sample B shows much more microbeads with fluorescence than Sample A. Sample C shows that almost all micro-beads are filled with the fluorescent HPTS and also shows more transparency because of the thinner layer. Sample D shows the best contrast and the different size of the particles can be clearly seen. All micro-beads are filled with fluorescent material. The samples with the highest amount of HPTS will also generate the highest fluorescent intensity, however the higher concentration of HPTS also causes higher absorption of the excitation signal. This may result a lower fluorescence and increasing the excitation signal power will cause more photobleaching. We have characterized the fluorescence in sample D but we did not include all results since the expected peak responsivity is at a much higher pH level than required for our application, as will be also shown in the measurement results of the next section.

C. Hydrogel analysis by Fluorescence Spectroscopy

The optical properties of the samples were investigated by transmission measurements in the range from 350 to 700 nm for the 4 types of layers using a Horiba Fluorlog-3 microscope. The 3-22 configuration was used in this research. The samples were submerged for several minutes in different pH solutions and placed in the spectrometer. The solutions were at a constant temperature around ambient temperature. The measured responses of Fig. 7 clearly show changes in emission as the pH changes. Especially when using an excitation wavelength of λ_l= 475 nm large changes in the fluorescent signal at λ_e= 525 nm can be observed when the pH changes.

The peak magnitude of the fluorescent signal at λ_e= 525 nm of sample B and C at λ_h= 475 nm and λ_l= 405 nm is shown in Fig. 7. A large dependence of the fluorescence on the pH of both sample B and C can be seen when excited at λ_h= 475 nm. In Fig. 7 can be also seen that around pH=7 sample B and sample C have a comparable sensitivity. This is due to the fact that the thicker sample B holds more active HPTS particles and sample C has a higher HPTS concentration. At λ_l= 405 nm source the fluorescent signal does not significantly vary with the pH. The small variations are probably due to mounting and remounting of the samples in the spectrometer after each pH measurement point. From all previous measurement results it was decided to use the fluorescent signal with illumination at λ_l= 405 nm as a reference level for each pH value as described in the next section.

VIII. Ratiometric Readout Technique

The presence of dual absorption bands in HPTS enables the use of dual excitation ratiometric detection as can be found in literature [26] [21]. The method is based in fact that the

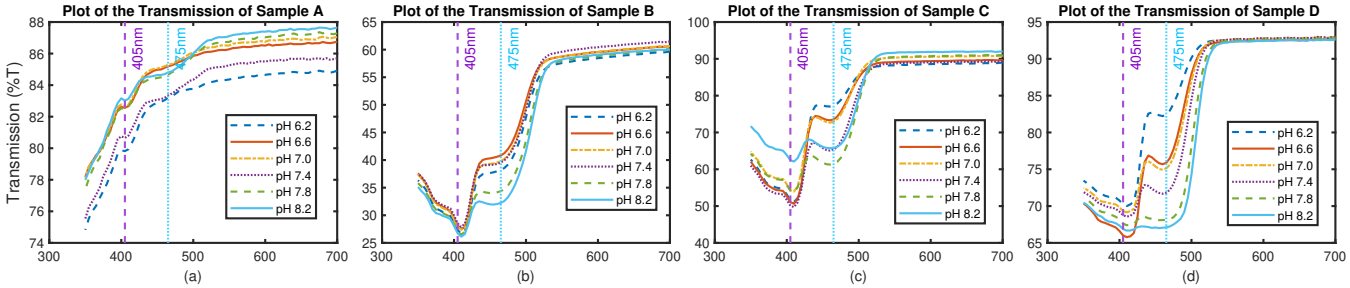

Fig. 4. From left to right: Transmittance of Sample A, B, C and D with varying pH and increasing HPTS concentrations.

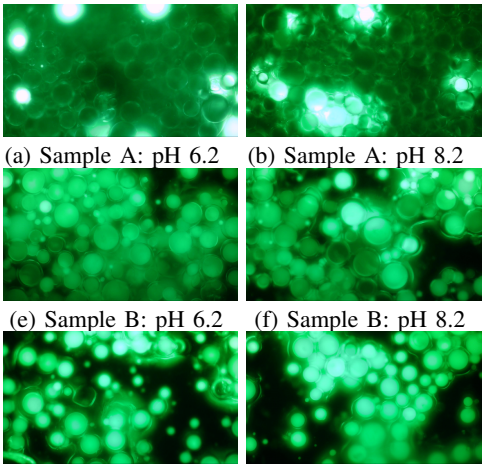

(a) Sample A: pH 6.2 (b) Sample A: pH 8.2

(e) Sample B: pH 6.2 (f) Sample B: pH 8.2

(g) Sample C: pH 6.2 (h) Sample C: pH 8.2

Fig. 5. Sample images of the Zeiss microscope with GFP filter and 20x magnification

ratio signal holds the dye concentration in both the numerator and the denominator, thus the concentration term cancels [27]. From the measurement results in Fig. 7 of the previous section it can be seen that the fluorescent signal at λ_h= 475 nm has a large dependence on the pH, while it does not vary with the pH at λ_h= 405 nm. Therefore the fluorescent signal at λ_l= 405 nm can be used as a reference level. Hence it was decided to use dual wavelength excitation at λ_h= 475 nm and λ_l= 405 nm and to calculate the ratio of these fluorescent signals to determine the pH. The method involves subsequent detection of the intensity E of the fluorescent signal at λ_e= 525 nm when illuminating the sample with λ_S= 405 and 475 nm respectively at a certain pH level. The ratio $\alpha(pH)$ is then calculated as

$$\alpha(pH) = \frac{E(pH)_{\lambda=475}}{E(pH)_{\lambda=405}}. \quad (3)$$

This method enables (first order) compensation of unwanted effects such as changes in the light path, stray light, background illumination and intensity loss by bleaching [26]. Dual band ratiometric detection also creates more standard curves [26]. The responsivity $R(pH)$ of the sensor for changes in pH can be written as

$$R(pH) = \frac{\delta\alpha(pH)}{\delta(pH)}. \quad (4)$$

The dual-wavelength ratiometric method can be easily implemented by first illuminating the sample using a LED with peak emission at λ_l= 405 and, after this, a LED with peak emission at λ_h= 475 nm. In both cases, the fluorescent response of the micro beads in the hydrogel layer at λ_d= 525 nm is measured by a spectrometer or a photo detector with a green filter. The measured spectra of the fluorescent signals and penetration depth at different pH levels provide enough insight for a prototype design as will be discussed in the next section.

IX. SENSOR PROTOTYPE DESIGN

In our application, the hydrogel layer needs to be in close contact with the heart on one side and the source and detector should be placed on the other side. The most straightforward way of measurement is therefore reflection mode. The measured average values of the absorption depth d_p over the whole pH range of the samples are given in Table I. These results show a low absorption at λ_d= 525 nm for all samples. A typical travel distance of L_{525}= 7 mm of the fluorescent signal in the hydrogel has been found by extrapolation using the absorption coefficient of the 1 mm layers, which indicates that collection of the fluorescent signal over a large area is possible. For the illumination sources λ_l= 405 nm and λ_h = 475 nm, the measured absorption is much higher and the resulting average penetration depths in the hydrogel have been found as L_{405}= 1mm and L_{475}= 2 mm respectively. The experiments also showed that the response time mainly depends on the layer thickness. For a reasonable speed in a real-time application, a layer less than 1 mm is required. As a compromise between mechanical strength and the response time, a typical thickness of the hydrogel layer of 0.5 mm or less would be favourable. The short penetration depth of the excitation light requires a design using orthogonal projection of the excitation sources on the hydrogel layer, while the fluorescent light at λ_d = 525 nm can be collected laterally over a larger distance.

Taking into account the demands for a multisensor system, usable for surgeons during an operation, two options for the realisation were considered. Thin optical probes (cannula) inserted at several locations in the tissue may be used where the hydrogel layer is mounted on the tip of the optical fibre bundles on the probes. Fibres guide the LED light into the hydrogel and others collect the fluorescent signal from the layer to a detector. In terms of optical design a better option would be the use of a planar sensor, held in place by a wire mesh around the heart. A MEMS (Micro Electro-Mechanical

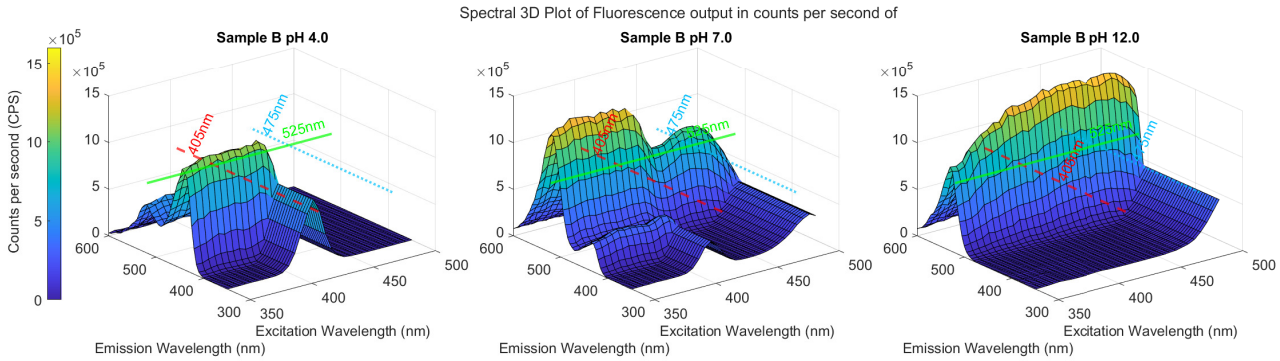

Fig. 6. Horiba Fluorlog spectral plots: Signal in counts per second of Sample B, From left to right pH = 4.0, pH = 7.0 and pH is 12.0

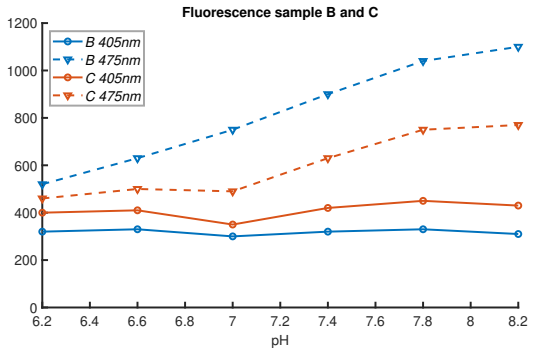

Fig. 7. Fluorescent signals of sample B and C at λ_l = 405 and 475 nm at different pH levels.

System) device realisation, as illustrated in Fig. 8, is proposed as a small planar sensor device.

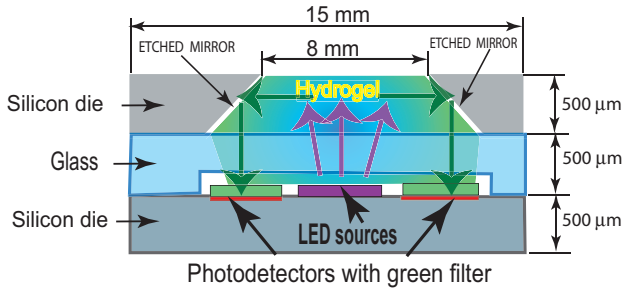

Fig. 8. Planar sensor configuration.

The illustration shows two silicon wafers, typical thickness of around 500 μm, bonded to a glass wafer in the middle . The top die has a cavity of typically a few square mm^2 filled with the hydrogel layer. The sidewalls are used as mirrors to collect the laterally fluorescent light onto photodetectors placed on the lower die. Optically flat 45° angle mirrors fabricated by anisotropic etching in silicon, based on our previous work [28] [29], can be used as highly reflective mirrors. Fabrication of such a lateral type of reflection probe has not been implemented yet. Such a prototype involves advanced processing and more costly and time consuming fabrication. However batch fabrication in commercial production however may decrease this cost dramatically. A less complicated, needle type of reflection prototype has been designed, tested and evaluated as described in the next section.

X. Prototype using a reflection probe

A reflection optical probe sensor has been implemented by mounting the hydrogel on a commercial probe as depicted in Fig. 9. Reflection probes are commercially available in many different types and sizes. Such a probe should be robust, yet thin in order not to damage the tissue. In the experiments, a

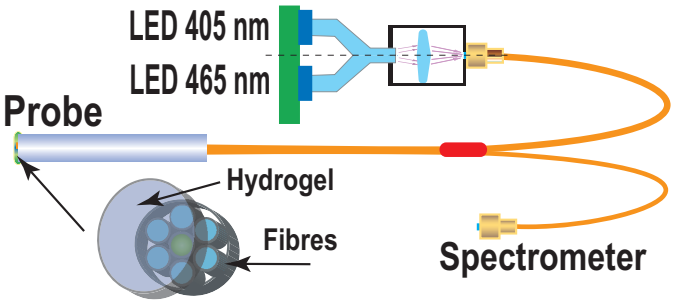

Fig. 9. Reflection probe with hydrogel measurement setup.

2mm Avantes FCR-7UVIR200-2-2.5×100 reflection probe, as illustrated in Fig. 9, has been used. Since the hydrogel does not adhere to the glass of the probe tip, a plastic holder was 3D printed for the tests. Hydrogel layers of 1mm and 0.5 mm thickness are sufficiently flexible to be wrapped around the tip of the holder on the probe and were held in place by a small O-ring, as can be seen in the photo of Fig.10.

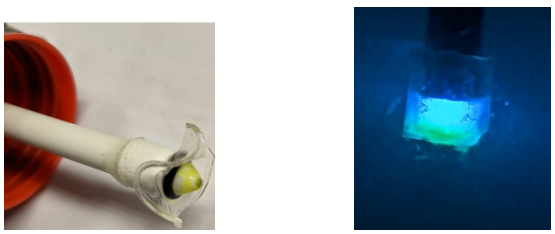

(a) Holder and 1mm hydrogel layer.

(b) Fluorescence in a 1mm hydrogel layer.

Fig. 10. Camera photos of the probe tip.

The probe enables easy interfacing to an Avantes Starline USB spectrometer and to the LED light sources using SMA

connectors. The light from the light source was guided through six 200 μm illumination fibres around a centre fibre to the sample. The single 200 μm fiber in the centre was connected to the spectrometer measuring the sample reflection. As excitation light sources, a Bivar UV5TZ-400-15 (405nm) LED and a blue Luxeon LXHL-PB01 (475nm) LED were used. The LED's can be individually switched on and off and are optically connected via a Y-shaped plastic light pipe and a lens to the other connector of the Avantes probe. The 475 nm LED operated at a constant current of 350 mA, producing an intensity of 15 W/m^2 on the hydrogel layer. The 405 nm LED operated at 20 mA and producing 16 W/m^2. The spectrometer was set for an integration time of 5ms and an averaging number of 1000.

A. Results using the reflection probe

Fig. 10b shows a 1 mm sensing layer on the probe after it had been just submerged in a pH solution. A clear layer of fluorescence can be observed at the surface where the buffer solution has diffused. Using the Avantes spectrometer in the setup of Fig.9 the emission spectra from 350-700 nm of several samples were recorded. From these spectra, the ratios of the fluorescent signal at λ_e = 525 nm at the two excitation wavelengths λ_{405} and λ_{465} were calculated. Fig. 11 shows the characteristic, sigmoid shaped, plots of the measured ratio α of Sample C as a function of pH. The measured signal ratio

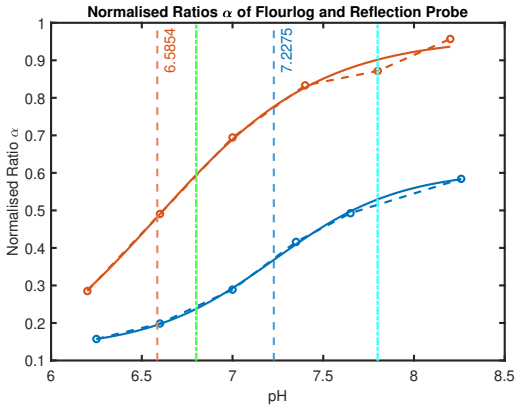

Fig. 11. Ratio α of the fluorescent signals of Sample B (red) C (blue) at different pH levels.

at the excitation wavelengths $R_{475/405}$ was fitted using the Boltzmann function

$$\mathrm{pH}(\alpha_{475/405}) = \frac{a-b}{1+e^{(\mathrm{R}_{475/405}-c)/d}} + b \qquad (5)$$

where a, b, c, and d are empirical parameters describing the initial value (a), final value (b), center (c) and the width of the fitting curve (d). The derived responsivity R for changes in pH, according to equation (4), is plotted in Fig. 12. The measurements using the probe type of sensor have shown a high sensitivity for changes in pH, due to the very high sensitivity of the HPTS dye [26]. The lower amount of HPTS in sample B results in a higher pKa value of the hydrogel material, resulting in a maximum responsivity of 52%/pH at

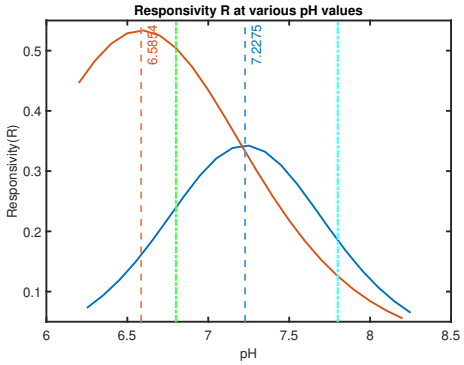

Fig. 12. Responsivity R of Sample B (red) C (blue) at different pH levels.

pH= 6.58 and for sample C 35%/pH at pH= 7.23. Sample B shows a larger maximum response than sample C, because more fluorescent signal is generated and collected in the larger thickness (1 mm) layer due the larger penetration depth. The pH range where highest responsivity occurs can be controlled by the amount of HPTS in the layer.

B. Response time measurement

The response time of the sensors depends on the diffusion speed of the hydrogen ions in the hydrogel layer. Fig. 13 shows

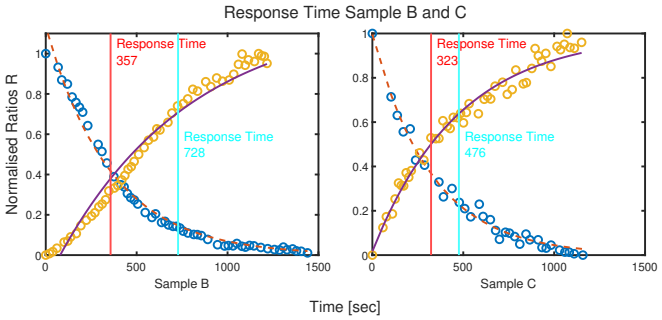

Fig. 13. Response time of Sample B (L=1.0 mm) and Sample C (L=0.5 mm).

the step response of the 0.5 mm and 1.0 mm layer probe by subsequent immersion into a pH= 6.2 and a pH= 8.2 buffer solution. The figure shows for Sample B a first-order response with a time constant around τ= 540s. For Sample C a first-order response with a typical time constant around τ= 350s.

C. Repeatability

In order to test the accuracy of the sensor after calibration, three measurements were done with the same buffer solutions at an ionic strength of 150 mM with 5 minutes waiting time in between. Fig. 14 shows the results of cycling the pH with a single probe. The plots show that the repeatability of the sensing layer is poor. The main reason for this is the low adhesion of the hydrogel to the probe surface resulting in detaching of the hydrogel layer from the probe surface and/or instability of the layer due to mechanical stress. Recently some techniques to improve the adhesion of wet hydrogels to smooth surfaces like glass have been described in literature [30].

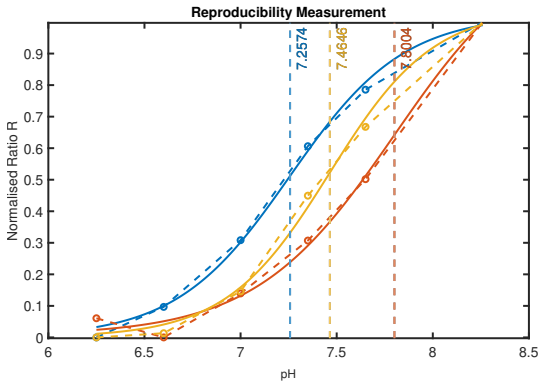

Fig. 14. Results of the repeatability measurements.

XI. Conclusions

This work presents an extensive optical characterization (transmission, absorption and fluorescence) of several types of hydrogel layers with HPTS (8-hydroxy-1,3,6-pyrene trisulfonic acid trisodium salt) embedded in micro-beads at different pH levels. From the optical characterization we selected a two-wavelength ratiometric type of measurement using low-cost LED's as favorable. Based on the optical characterisation of different hydrogel layer samples excitation of the HPTS dye using LED's emitting at wavelengths of λ_e= 405 and 475 nm and detection of the fluorescent signal was implemented using a thin reflection probe. The pH level was calculated as the ratio at the peak of the fluorescent signal at λ_d= 525 nm at both excitation wavelengths. In terms of response time in our application a suitable hydrogel layer thickness was found at 0.5 mm. Increasing the layer thickness to 1mm increased both the response time and the sensitivity. For the intended application for the detection of myocardial ischaemia we have tested several hydrogel layers using a thin reflection probe as a pH sensor. We have characterized several HPTS hydrogel layers in reflection mode in liquids. The probe prototype has shown a high sensitivity and a good selectivity for pH, however the reproducibility of the device needs to be improved before performing further experiments. At the moment, the accuracy is limited due to the low adhesion of the hydro-gel to the small surface of the glass of the probe. New processing techniques to improve this need to be tested. A novel reflection type of prototype using the same layers has been proposed in section IX. This planar device has a more efficient light coupling and a sensing area of about two orders of magnitude higher, enabling much more signal power. Improved control of the thickness of the layer and a better mechanical coupling to the heart tissue is also expected from such a prototype. Therefore future work we plan to develop lateral devices on bulk micromachined MEMS substrates using the 0.5 mm hydrogel layers as presented here for future work. Future experiments using these new prototypes are needed to study the effect of cardioplegia on pH measurement. There are many types of cardioplegia and all these solutions have high levels of potassium chloride (KCl) and other electrolytes which may result in changes in the responsivity due to a change in ionic strength in the sensing layer. Finally, in vivo experiments are required to demonstrate the performance of the devices in the actual application.

Acknowledgments

The authors gratefully acknowledge Drs. Michiel Vriesendorp of the Thoracic Surgery Department, Leiden University Medical Centre, Leiden, The Netherlands for his advice on the medical and practical aspects of open heart surgery and Ing. Stefaan Heirman from the Photovoltaic Materials and Devices Group of Delft University of Technology for his advice and help on the optical characterization of the layers and the fluorescence microscope measurements.

References

[1] C. Carvajal, A. Goyal, and P. Tadi, *Cardioplegia*. StatPearls Publishing, 3 2020.

[2] G. P. Dobson, G. Faggian, F. Onorati, and J. Vinten-Johansen, "Hyperkalemic cardioplegia for adult and pediatric surgery: end of an era?" *Frontiers in Physiology*, vol. 4, p. 228, 8 2013.

[3] Glenn P. Gravlee, *Cardiopulmonary Bypass: Principles and Practice*. Wolters Kluwer Health, 2008.

[4] C. Drescher, A. Diestel, S. Wollersheim *et al.*, "How does hypothermia protect cardiomyocytes during cardioplegic ischemia?" *European Journal of Cardio-thoracic Surgery*, vol. 40, no. 2, pp. 352–359, 1 2011.

[5] A. T. Turer and J. A. Hill, "Pathogenesis of myocardial ischemia-reperfusion injury and rationale for therapy," pp. 360–368, 8 2010.

[6] C. H. Lee, M. H. Ju, J. B. Kim *et al.*, "Myocardial injury following aortic valve replacement for severe aortic stenosis," *Korean Journal of Thoracic and Cardiovascular Surgery*, vol. 47, no. 3, pp. 233–239, 2014.

[7] C. Steenbergen and N. G. Frangogiannis, "Ischemic heart disease," in *Muscle*. Elsevier, 2012, pp. 495–521.

[8] S. Pischke, S. Hyler, C. Tronstad *et al.*, "Myocardial tissue CO_2 tension detects coronary blood flow reduction after coronary artery bypass in real-time †," *British Journal of Anaesthesia*, vol. 114, no. 3, pp. 414–422, 3 2015.

[9] A. Steinegger, O. S. Wolfbeis, and S. M. Borisov, "Optical Sensing and Imaging of pH Values: Spectroscopies, Materials, and Applications," pp. 12 357–12 489, 11 2020.

[10] M. F. Vriesendorp, "Detecting myocardial ischaemia with optochemical sensing by using a fluorescent hydrogel," Master's thesis, Delft University of Technology, Delft, 2021.

[11] H. El Banani, M. Bernard, D. Baetz *et al.*, "Changes in intracellular sodium and pH during ischaemia-reperfusion are attenuated by trimetazidine: Comparison between low- and zero-flow ischaemia," *Cardiovascular Research*, vol. 47, no. 4, pp. 688–696, 9 2000.

[12] G. X. Yan and A. G. Kléber, "Changes in extracellular and intracellular pH in ischemic rabbit papillary muscle," *Circulation Research*, vol. 71, no. 2, pp. 460–470, 1992.

[13] J. J. Lemasters, J. M. Bond, E. Chacon *et al.*, "The pH paradox in ischemia-reperfusion injury to cardiac myocytes." *EXS*, vol. 76, pp. 99–114, 1996.

[14] S. F. Khuri and W. A. Marston, "On-line metabolic monitoring of the heart during cardiac surgery," *Surgical Clinics of North America*, vol. 65, pp. 439–453, 1985.

[15] K. R. Khabbaz, F. Zankoul, and K. G. Warner, "Intraoperative metabolic monitoring of the heart: II. Online measurement of myocardial tissue pH," *Annals of Thoracic Surgery*, vol. 72, no. 6, pp. S2227–S2233, 12 2001.

[16] S. E. Pischke, C. Tronstad, L. Holhjem *et al.*, "Perioperative detection of myocardial ischaemia/reperfusion with a novel tissue CO2 monitoring technology," *European Journal of Cardio-thoracic Surgery*, vol. 42, no. 1, pp. 157–163, 2012.

[17] P. Atkins and J. d. Paula, *Atkins' Physical chemistry*. Oxford University Press, 2006.

[18] S. P. Nichols, M. K. Balaconis, R. M. Gant *et al.*, "Long-term in vivo oxygen sensors for peripheral artery disease monitoring." Springer NY LLC, 2018, vol. 1072, pp. 351–356.

[19] D. Wencel, A. Kaworek, T. Abel *et al.*, "Optical Sensor for Real-Time pH Monitoring in Human Tissue," *Small*, vol. 14, no. 51, p. 1803627, 12 2018.

[20] J. Gong, M. G. Tanner, S. Venkateswaran *et al.*, "A hydrogel-based optical fibre fluorescent pH sensor for observing lung tumor tissue acidity," *Analytica Chimica Acta*, vol. 1134, pp. 136–143, 10 2020.
[21] S. Cattini, L. Accorsi, S. Truzzi, and L. Rovati, "On the Development of an Instrument for In-Line and Real-Time Monitoring of Blood-pH in Extracorporeal Circulation," *IEEE Transactions on Instrumentation and Measurement*, vol. 69, no. 8, pp. 5640–5648, 8 2020.
[22] Z. H. Meng, "Molecularly Imprinted Sol-Gel Sensors," in *Molecularly Imprinted Sensors*, 1 2012, pp. 303–337.
[23] X. Ge, Y. Kostov, and G. Rao, "High-stability non-invasive autoclavable naked optical CO 2 sensor," *Biosensors and Bioelectronics*, vol. 18, no. 7, p. 857–865, 2003.
[24] H. Kermis, Y. Kostov, P. Harms *et al.*, "Dual Excitation Ratiometric Fluorescent pH Sensor for Noninvasive Bioprocess Monitoring: Development and Application," *Biotechnology Progress*, no. 5, pp. 1047–1053, 2002.
[25] M. Born and E. Wolf, *Principles of Optics: Electromagnetic Theory of Propagation, Interference and Diffraction of Light*, 7th ed. Cambridge University Press, 1999.
[26] A. Chandra et al., "Highly Sensitive Fluorescent pH Microsensors Based on the Ratiometric Dye Pyranine Immobilized on Silica Microparticles," *Chemistry–A European Journal*, vol. 27, no. 53, pp. 13 279–13 279, 2021.
[27] M. Renganathan, E. Pfündel, and R. A. Dilley, "Thylakoid lumenal ph determination using a fluorescent dye: Correlation of lumen ph and gating between localized and delocalized energy coupling," *Biochimica et Biophysica Acta (BBA) - Bioenergetics*, vol. 1142, no. 3, pp. 277–292, 1993.
[28] D. B. Xu, "Fabrication of an ultraviolet absorption spectroscopy probe for protein quantification in bioreactors," Master's thesis, Delft University of Technology, Delft, 2017.
[29] N. P. Ayerden, M. Ghaderi, and R. F. Wolffenbuttel, "Design and fabrication of 45° inclined mirrors for wafer-level optical absorption spectroscopy," vol. 757, no. 1, 2016, Conference paper.
[30] H. Yuk et al., "Tough bonding of hydrogels to diverse non-porous surfaces," *Nat. Mater*, no. 15, pp. 190–196, 2016.

Ger de Graaf (M'98) was born in Delft, The Netherlands, in 1955. He is a research and teaching staff member at the Faculty of Electrical Engineering, Delft University of Technology. He received the B.E. degree in electrical and control engineering from the Hogeschool Rotterdam in the Netherlands, in 1983. He has owned a consultancy company specializing in computer measurement systems from 1992-1996. He received his Ph.D. degree at Delft University of Technology in 2008. He is a (co-)author of around 150 scientific publications and main author of around 30 international scientific papers since 1988. He is a member of the IEEE and holds one patent. His current research interests include infrared detection, optical spectrometry, MEMS, analog electronic circuits, sensors and micro-fabrication in general.

Maurits F. Vriesendorp was born in Tilburg, the Netherlands. He received his BSc in Clinical Technology from Leiden, Erasmus and Delft University in 2018 and his MSc in Biomedical Engineering from the Technical University Delft in 2021. During his Masters, he did a research internship at Stellenbosch university. Currently working as Business Analyst at Philips Engineering Solutions.

Hitham Mahmoud Amin Hassan was born in Egypt. He received his B.Sc. in chemistry from the Faculty of Science of Zagazig University, Egypt. In 2009 he obtained his M.Sc. and in 2013 his PhD in chemical engineering and materials science from Autonomous University of Madrid, Spain. He worked as a researcher at the Spanish National Research Council (CSIC) from 2008-2014 and after this as a post-doc at Polytechnic University of Milan. In 2017 he joined Else Kooi Lab of Delft University of Technology. He is also a lecturer at the chemistry department of Zagazig University. His main research focus is on wet and polymer processing developments for MEMS devices, such as for Organ-on-a-Chip, flexible devices and electrochemical sensors.

Paddy French received his B.Sc. in mathematics and M.Sc. in electronics from Southampton University, UK, in 1981 and 1982, respectively. In 1986 he obtained his Ph.D., also from Southampton University, which was a study of the piezoresistive effect in polysilicon. After 18 months as a post doc at Delft University, The Netherlands, he moved to Japan in 1988. For 3 years he worked on sensors for automotive at Nissan Motor Company. He returned to Delft University in May 1991 and was a staff member of the Laboratory for Electronic Instrumentation until 2019 when he moved to the Bioelectronics Laboratory. In 1999 he was awarded the Antoni van Leeuwenhoek chair and was from 2002 to 2012 head of the Electronic Instrumentation Laboratory. He was Editor-in-chief of Sensors and Actuators A and General Editor of Sensors and Actuators A&B from 2002-2018. His research interests are integrated sensor systems, micromachining, in particular for medical applications.